

Uncertainty modeling in 3D SEM stereophotogrammetry

Original

Uncertainty modeling in 3D SEM stereophotogrammetry / Carli, L., Galetto, M., Genta, G.. - STAMPA. - Series on Advances in Mathematics for Applied Sciences, 84:(2012), pp. 66-73. (AMCTM 2011 International Conference on Advanced Mathematical and Computational Tools in Metrology and Testing Göteborg (SWE) 20-22 June 2011) [10.1142/9789814397957_0009].

Availability:

This version is available at: 11583/2497024 since:

Publisher:

World Scientific

Published

DOI:10.1142/9789814397957_0009

Terms of use:

This article is made available under terms and conditions as specified in the corresponding bibliographic description in the repository

Publisher copyright

(Article begins on next page)

UNCERTAINTY MODELING IN 3D SEM STEREOPHOTOGRAMMETRY

LORENZO CARLI

*Department of Mechanical Engineering, Technical University of Denmark (DTU),
Produktionstorvet, Building 425, 2800 Kongens Lyngby, Denmark*

MAURIZIO GALETTO, GIANFRANCO GENTA

*Department of Production Systems and Business Economics, Politecnico di Torino,
Corso Duca degli Abruzzi 24, 10129 Torino, Italy*

The scanning electron microscope (SEM) is widely used to acquire high resolution images. In order to reconstruct the third dimension of surface features, photogrammetry methods can be adopted. A specimen is imaged in the SEM acquiring two images, the *stereo-pair*, by scanning the same area from two different perspectives. The stereo-matching problem is solved by area- or feature-based methods implemented in commercial software. Piazzesi provided a first model for deriving surface topography from eucentric stereo-pairs. An uncertainty evaluation for the vertical elevation has been performed in a recent work for a cylindrical item. The aim of the present work is to extend the uncertainty evaluation to all surface coordinates. The proposed approach is based on the multivariate law of propagation of uncertainty (MLPU). Some preliminary results are also presented and discussed.

Keywords: SEM, photogrammetry, stereo-pair technique, MLPU

1. Introduction

The scanning electron microscope (SEM) has some unique properties that, combined together, are matched by no other kind of microscope. It allows image ranges from 1 mm^2 to $1 \text{ }\mu\text{m}^2$ with an ultimate resolution of about 1 nm , comparable to the scanning probe microscope (SPM). Furthermore, the SEM is very promising for measuring surfaces having high aspect ratios. Main application areas are the semiconductor industry, life sciences, materials research and many industrial fields related to nanotechnology.

Nevertheless, many developments are still needed in order to transform the usage of SEMs into a technique where the complete topography of a surface can be determined by a truly 3D characterization, developing metrologically correct techniques and producing traceable measurement results. SEM images are purely two dimensional; a possible way to overcome this limitation is to the use

SEM in conjunction with image processing of stereographs [1]. This method, called the 3D-SEM technique, is based on photogrammetry and allows reconstruction of the third dimension of surface features. It has been extensively studied starting from the theoretical description given by Piazzesi [2].

This measuring procedure, together with relevant uncertainty evaluation, was examined in the case of a cylindrical item [3]: a wire gauge from TESA Technology with an external calibrated diameter of $250\ \mu\text{m}$. It can be positioned and fixed horizontally to the SEM stage to perform eucentric tilting; multiple views of the item can be acquired at different tilt angles. Another possibility is, instead, to position and clamp the cylindrical object vertically on the SEM stage, and then to tilt it by 90° . In this case, multiple views of the item can be obtained by performing rotations along the main axis of the cylinder. Figure 1 shows the moving stage of the SEM employed.

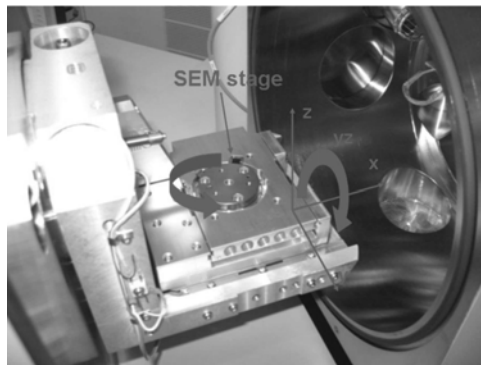


Figure 1. SEM Inspect 'S' stage, from FEI company, enabling translations along x , y and z -axis, yz tilt and rotation around the z -axis [3].

The aim of this work is to extend the uncertainty evaluation of stereo-pair reconstructions implemented in [3], relative to both tilting and rotation strategies, allowing for correlation between the input quantities of the measurement model.

2. Basic Principles of 3D SEM Stereophotogrammetry

To produce a stereoscopic reconstruction, a specimen is imaged in the SEM acquiring two images, the *stereo-pair*, by scanning the same area from two different perspectives, achieved by eucentric tilt of the sample. The image-matching problem mainly encompasses automatic identification in the stereo-pair of homologous points, representative of corresponding features. Nowadays

this procedure is performed using commercial software where the stereo-matching is done using an area- or a feature-based method [4]. In most SEMs, it is possible to take the two different stereo viewpoints by tilting the specimen about a horizontal axis x . Assuming that the surface region on the x -axis is brought into focus, the SEM focal plane then coincides with the reference xy -coordinate plane. The stereo-pair technique may be defined using the geometrical definitions given in Figure 2; further details are given in [5].

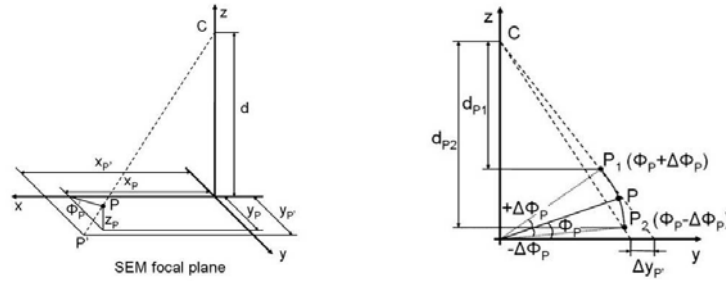


Figure 2. Geometrical definitions relative to a point P on the specimen surface. The working distance d is not shown to scale (under scaled) for ease of interpretation [5].

Piazzesi [1] provided a model for deriving surface topography from eucentric stereo-pairs, exploiting the physical P coordinates (ξ, η, z) . Subsequently, Bariani *et al.* [6] simplified this model fixing the constraint $d_1=d_2=d$, i.e. constant working distance between the two images. The equation for the z -coordinate has been further rewritten in [3] assuming that the distance between two points in a digital picture is given by the number of pixels n counted between the two points multiplied by the single pixel dimension (pixel size) p . Proceeding similarly for ξ - and η - coordinates gives

$$\left\{ \begin{array}{l}
z = \frac{p(n_{y1} - n_{y2}) \cos \Delta\varphi + \frac{2p^2 n_{y1} n_{y2}}{d} \sin \Delta\varphi}{\left(1 + \frac{p^2 n_{y1} n_{y2}}{d^2}\right) \sin 2\Delta\varphi + p \frac{n_{y1} - n_{y2}}{d} \cos 2\Delta\varphi} \\
\xi = \frac{2d - 2z \cos \Delta\varphi}{\frac{d}{p} \left(\frac{1}{n_{x1}} + \frac{1}{n_{x2}}\right)} \\
\eta = \frac{p(n_{y1} + n_{y2})(z \cos \Delta\varphi - d)}{p(n_{y1} - n_{y2}) \sin \Delta\varphi - 2d \cos \Delta\varphi}
\end{array} \right. \quad (1)$$

where the indices 1 and 2 refer, respectively, to the first image (tilted by an amount $-\Delta\varphi$) and the second image (tilted by an amount $+\Delta\varphi$) being used for the calculation.

A theoretical uncertainty evaluation for the z -coordinate, according to GUM [7], has been performed in [3] starting from Eq. (1), considering p , n_{y1} , n_{y2} , d and $\Delta\varphi$ as independent variables. It has been checked that a linear approximation of the measurement function is acceptable within the range of variation of input quantities. Furthermore, in a first approximation, the hypothesis of non-correlation among input quantities has been made based on empirical considerations [3].

The aim of this work is to extend the uncertainty evaluation to the vector $(z, \xi, \eta)^T$, considering the possible presence of correlations among input quantities.

3. Propagation of Uncertainties

System (1) can be formally written as follows:

$$Y = f(\mathbf{X}), \quad (2)$$

where the vector of input quantities is

$$\mathbf{X} = \left(p \quad n_{x1} \quad n_{x2} \quad n_{y1} \quad n_{y2} \quad d \quad \Delta\varphi \right)^T, \quad (3)$$

while the vector of output quantities is

$$\mathbf{Y} = (z \quad \xi \quad \eta)^\top. \quad (4)$$

The uncertainty corresponding to \mathbf{Y} may be estimated using the multivariate law of propagation of uncertainty (MLPU) described in [8], following the lines of GUM [7]. The covariance matrix $\hat{\Sigma}_Y$ associated with the estimate $\hat{\mathbf{Y}}$ is given by

$$\hat{\Sigma}_Y = \mathbf{J} \hat{\Sigma}_X \mathbf{J}^\top, \quad (5)$$

where $\hat{\Sigma}_X$ is the covariance matrix associated with the estimate $\hat{\mathbf{X}}$ and \mathbf{J} is the Jacobian of $f(\mathbf{X})$ evaluated at $\hat{\mathbf{X}}$. Due to the difficulty in obtaining analytical expressions of the partial derivatives of f , \mathbf{J} is approximated numerically. The covariance matrix is assigned according to GUM; for each pair of estimates x_i and x_j of input quantities, the covariance $u(x_i, x_j)$ is related to the uncertainties $u(x_i)$ and $u(x_j)$ through the relation

$$u(x_i, x_j) = \rho_{ij} u(x_i) u(x_j), \quad (6)$$

where ρ_{ij} is the correlation coefficient for the estimates.

4. Evaluation of Uncertainty Contributions

The cases of uncorrelated input quantities (section 4.1) and correlated input quantities (section 4.2) have been both considered for the application described in previous sections [3].

4.1. Uncorrelated Input Quantities

According to the hypothesis in [3], as a first approximation, the covariance matrix associated with \mathbf{X} can be reduced to the following diagonal matrix:

$$\hat{\Sigma}_X = \begin{bmatrix} u^2(p) & 0 & 0 & 0 & 0 & 0 & 0 \\ 0 & u^2(n_{x1}) & 0 & 0 & 0 & 0 & 0 \\ 0 & 0 & u^2(n_{x2}) & 0 & 0 & 0 & 0 \\ 0 & 0 & 0 & u^2(n_{y1}) & 0 & 0 & 0 \\ 0 & 0 & 0 & 0 & u^2(n_{y2}) & 0 & 0 \\ 0 & 0 & 0 & 0 & 0 & u^2(d) & 0 \\ 0 & 0 & 0 & 0 & 0 & 0 & u^2(\Delta\varphi) \end{bmatrix}. \quad (7)$$

Since the same considerations apply to the numbers of pixels relevant to coordinates x and y , it has been assumed that:

$$u(n_{x1}) = u(n_{x2}) = u(n_{y1}) = u(n_{y2}). \quad (8)$$

Uncertainty evaluation for the cylindrical item, relative to both tilting and rotation strategies, reported in tabular form in [3], is now rewritten in matrix form. In the case of rotation, the covariance matrix associated with \mathbf{X} results

$$\hat{\Sigma}_x = \begin{bmatrix} 7.72 \cdot 10^{-18} & 0 & 0 & 0 & 0 & 0 & 0 \\ 0 & 1.00 \cdot 10^{-2} & 0 & 0 & 0 & 0 & 0 \\ 0 & 0 & 1.00 \cdot 10^{-2} & 0 & 0 & 0 & 0 \\ 0 & 0 & 0 & 1.00 \cdot 10^{-2} & 0 & 0 & 0 \\ 0 & 0 & 0 & 0 & 1.00 \cdot 10^{-2} & 0 & 0 \\ 0 & 0 & 0 & 0 & 0 & 4.69 \cdot 10^{-7} & 0 \\ 0 & 0 & 0 & 0 & 0 & 0 & 2.08 \cdot 10^{-6} \end{bmatrix}, \quad (9)$$

while in the case of tilt

$$\hat{\Sigma}_x = \begin{bmatrix} 1.18 \cdot 10^{-17} & 0 & 0 & 0 & 0 & 0 & 0 \\ 0 & 1.00 \cdot 10^{-2} & 0 & 0 & 0 & 0 & 0 \\ 0 & 0 & 1.00 \cdot 10^{-2} & 0 & 0 & 0 & 0 \\ 0 & 0 & 0 & 1.00 \cdot 10^{-2} & 0 & 0 & 0 \\ 0 & 0 & 0 & 0 & 1.00 \cdot 10^{-2} & 0 & 0 \\ 0 & 0 & 0 & 0 & 0 & 3.22 \cdot 10^{-7} & 0 \\ 0 & 0 & 0 & 0 & 0 & 0 & 3.57 \cdot 10^{-6} \end{bmatrix}. \quad (10)$$

Units of the International System (SI), without any multiples or submultiples, are used in the two previous, and in all subsequent, equations. Calculations have been performed for the item in a particular position of the measurement space. However, as a first approximation, values of $\hat{\Sigma}_x$ can be assumed to be the same for the whole measurement space.

Applying Eq. (5), i.e. MLPU, in the case of rotation gives

$$\hat{\Sigma}_y = \begin{bmatrix} 9.90 \cdot 10^{-12} & 1.16 \cdot 10^{-12} & 1.13 \cdot 10^{-12} \\ 1.16 \cdot 10^{-12} & 1.18 \cdot 10^{-12} & 1.19 \cdot 10^{-12} \\ 1.13 \cdot 10^{-12} & 1.19 \cdot 10^{-12} & 1.19 \cdot 10^{-12} \end{bmatrix}, \quad (11)$$

while in the case of tilt

$$\hat{\Sigma}_y = \begin{bmatrix} 1.32 \cdot 10^{-11} & 1.17 \cdot 10^{-12} & 1.13 \cdot 10^{-12} \\ 1.17 \cdot 10^{-12} & 1.15 \cdot 10^{-12} & 1.16 \cdot 10^{-12} \\ 1.13 \cdot 10^{-12} & 1.16 \cdot 10^{-12} & 1.17 \cdot 10^{-12} \end{bmatrix}. \quad (12)$$

4.2. Correlated Input Quantities

Considering now the possible presence of correlation, based on the physics of the process, the following covariance matrix associated with \mathbf{X} should be adopted:

$$\hat{\Sigma}_{\mathbf{X}} = \begin{bmatrix} u^2(p) & 0 & 0 & 0 & 0 & 0 & 0 \\ - & u^2(n_{x1}) & 0 & 0 & 0 & 0 & 0 \\ - & - & u^2(n_{x2}) & 0 & 0 & 0 & 0 \\ - & - & - & u^2(n_{y1}) & u(n_{y1}, n_{y2}) & u(n_{y1}, d) & u(n_{y1}, \Delta\varphi) \\ - & - & - & - & u^2(n_{y2}) & u(n_{y2}, d) & u(n_{y2}, \Delta\varphi) \\ - & - & - & - & - & u^2(d) & 0 \\ - & - & - & - & - & - & u^2(\Delta\varphi) \end{bmatrix}. \quad (13)$$

Elements below the main diagonal of $\hat{\Sigma}_{\mathbf{X}}$ in Eq. (13) are not displayed since it is a symmetric matrix.

For non-zero terms not on the main diagonal, it is assumed complete correlation ($|\rho_{ij}|$ equal to 1). The signs of the correlation coefficients were obtained, as a first approximation, using the functional relationships between the variables and previous experimental analysis. Eq. (13) becomes

$$\hat{\Sigma}_{\mathbf{X}} = \begin{bmatrix} u^2(p) & 0 & 0 & 0 & 0 & 0 & 0 \\ - & u^2(n_{x1}) & 0 & 0 & 0 & 0 & 0 \\ - & - & u^2(n_{x2}) & 0 & 0 & 0 & 0 \\ - & - & - & u^2(n_{y1}) & +u(n_{y1})u(n_{y2}) & -u(n_{y1})u(d) & +u(n_{y1})u(\Delta\varphi) \\ - & - & - & - & u^2(n_{y2}) & +u(n_{y2})u(d) & -u(n_{y2})u(\Delta\varphi) \\ - & - & - & - & - & u^2(d) & 0 \\ - & - & - & - & - & - & u^2(\Delta\varphi) \end{bmatrix}. \quad (14)$$

Applying Eq. (5), i.e. MLPU, in the case of rotation gives

$$\hat{\Sigma}_{\mathbf{Y}} = \begin{bmatrix} 7.02 \cdot 10^{-12} & 1.13 \cdot 10^{-12} & 1.11 \cdot 10^{-12} \\ 1.13 \cdot 10^{-12} & 1.18 \cdot 10^{-12} & 1.19 \cdot 10^{-12} \\ 1.11 \cdot 10^{-12} & 1.19 \cdot 10^{-12} & 1.20 \cdot 10^{-12} \end{bmatrix}, \quad (15)$$

while in the case of tilt

$$\hat{\Sigma}_{\mathbf{Y}} = \begin{bmatrix} 1.30 \cdot 10^{-11} & 1.17 \cdot 10^{-12} & 1.01 \cdot 10^{-12} \\ 1.17 \cdot 10^{-12} & 1.15 \cdot 10^{-12} & 1.16 \cdot 10^{-12} \\ 1.01 \cdot 10^{-12} & 1.16 \cdot 10^{-12} & 1.18 \cdot 10^{-12} \end{bmatrix}. \quad (16)$$

5. Final Remarks

The proposed approach based on MLPU is simple and completely automatic, furthermore it takes into account covariance contributions.

Both in the case of uncorrelated input quantities (Eq. (11) and (12)) and in the case of correlated input quantities (Eq. (15) and (16)), according to the geometry of the problem (Figure 2), variance contributions for ζ and η are lower than those for z by about one order of magnitude. Moreover, covariance contributions are always comparable with the variance contributions for ζ and η .

The inclusion of terms representing correlation between the input quantities leads to the variance contribution for z being lower in case of rotation (Eq. (11) and (15)).

References

1. H. Sato, A way to measurement for submicron meter: surface profile by scanning electron microscope, *Proc. Manufacturing International* 63–73 (1990).
2. G. Piazzesi, Photogrammetry with the scanning electron microscope, *J. Phys. E: Sci. Instrum.* 6:392–396 (1973).
3. L. Carli, G. Genta, A. Cantatore, G. Barbato, L. De Chiffre and R. Levi, Uncertainty evaluation for three-dimensional scanning electron microscope reconstructions based on the stereo-pair technique, *Meas. Sci. Technol.* 22:035103 (2011).
4. D. Scharstein and R. Szeliski, A taxonomy and evaluation of dense two-frame stereo correspondence algorithms, *Int. J. Comput. Vision.* 47:7–42 (2002).
5. F. Marinello, P. Bariani, E. Savio, A. Horsewell and L. De Chiffre, Critical factors in SEM 3D stereo microscopy, *Meas. Sci. Technol.* 19:065705 (2008).
6. P. Bariani, L. De Chiffre, H.N. Hansen and A. Horsewell, Investigation on the traceability of three-dimensional scanning electron microscope measurements based on the stereo-pair technique, *Precis. Eng.* 29:219–228 (2005).
7. JCGM 100:2008, Evaluation of measurement data - Guide to the expression of uncertainty in measurement (GUM) (2008).
8. F. Franceschini, M. Galetto, D. Maisano, L. Mastrogiacomo and B. Pralio, *Distributed Large-Scale Dimensional Metrology*, London: Springer (2011).